

ANALYSIS OF 3D PLANAR CRACKS WITH CONSIDERATION OF SURFACE STRESS EFFECTS

Thai Binh Nguyen¹, Jaron Rungamornrat²,
Teerapong Senjuntichai³, and Anil Wijeyewickrema⁴

^{1,2,3}Department of Civil Engineering, Faculty of Engineering, Chulalongkorn University, Bangkok, Thailand

⁴Department of Civil and Environmental Engineering, Tokyo Institute of Technology, Tokyo, Japan
e-mail: Binh.T@student.chula.ac.th¹, Jaron.R@chula.ac.th², Teerapong.S@chula.ac.th³,
wijeyewickrema.a.aa@m.titech.ac.jp⁴

Received Date: February 27, 2014

Abstract

An efficient numerical procedure for modeling planar cracks in three-dimensional, linear elastic, infinite media accounting for the surface stress effect is presented in this paper. The concept of surface stresses, which has been widely employed in the modeling of nano-scale problems, is considered in the present study to derive a suitable mathematical model capable of simulating nano-sized cracks. An infinitesimally thin layer of material on the crack surface is modeled by a surface with zero-thickness and perfectly adhered to the bulk material, with its behavior governed by the Gurtin-Murdoch constitutive law. In the formulation, the classical theory of isotropic linear elasticity is utilized to establish the governing equation of the bulk material in terms of completely regularized boundary integral equations for the displacements and tractions on the crack surface. For the zero-thickness layer, the final governing equation incorporating the surface stress effect is obtained in a weak form following the standard weighted residual technique. Solutions of the fully coupled system of equations are then obtained by the FEM-SGBEM coupling numerical procedure. Owing to the weakly singular feature of all involved boundary integral equations, standard C^0 interpolation functions are used everywhere in the approximation of crack-face data and only special quadrature for evaluating nearly singular and weakly singular integrals is required. Once the implemented numerical scheme is validated with available benchmark solutions, it is applied to investigate the nano-scale influence of nano-sized cracks. Results from an extensive parametric study reveal that, the presence of surface stresses not only increases the near-surface material stiffness but also introduces size-dependent behavior of predicted solutions and the reduction of stresses in the region ahead of the crack front.

Keywords: FEM-SGBEM coupling, Gurtin-Murdoch model, Nano-sized cracks, Size dependency, Surface stresses

Introduction

Nano-structured materials such as nano-belts, nano-springs, nano-wires, nano-tubes, and nano-composites have received much attention in various fields in recent years due to their desirable and unique features. One obvious example of their vast applications is the invention of nano-scale components and devices. In the design procedure, analysis and assessment of failure/damage have been found to be an essential step that must be properly considered to ensure the safety and integrity throughout their lifespan. While conventional linear elastic fracture mechanics has been well established and successfully employed as a tool in the modeling of existing defects/flaws in linear elastic media at a macroscopic scale, those hypothetical models have failed to simulate the problem of nano-sized cracks due to the limitation of their underlying governing physics and simplified assumptions. The enhancement of classical continuum-based fracture models to properly incorporate the nano-scale influence is, therefore, required in order to accurately capture inherent physical

characteristics at such a small scale. Atomistic and molecular dynamics simulations have demonstrated that atoms in the vicinity of the free surface behave differently from those within the bulk material and effects of the surface free energy on the mechanical behavior can be very important at the nano-scale level. This near-surface phenomenon is one of the most important factors rendering the difference between macroscopic and nano-scale structures and must be suitably incorporated into the continuum-based models.

Gurtin and Murdoch [1] and Gurtin et al. [2] proposed a well-known, surface elasticity, continuum-based theory to enhance the modeling capability to capture the effects of surface energy in solid materials. In such model, the surface is assumed to be elastic and very thin, which can be mathematically modeled as a zero-thickness layer fully bonded to the remaining bulk part. The behavior of such an idealized surface is described by a linear constitutive relation involving surface material parameters different from those of the bulk material. In the past two decades, the surface elasticity theory proposed by Gurtin and Murdoch has been extensively utilized to examine various nano-scale problems (e.g., nano-scale elastic films [3-5], nano-sized particles and wires [4], nano-scale inhomogeneities [6-8], nano-indentations [9], etc.) and has also been validated because results predicted by this continuum-based model exhibit reasonably good agreement with those from atomistic and molecular dynamics simulations [4,10-12].

The Gurtin-Murdoch model has also been utilized in the investigation of nano-sized cracks; however, based on a careful literature review, most existing studies are still limited to certain problem settings, formulations and solution techniques. For instance, studies of nano-sized cracks under various loading conditions using either the two-dimensional, blunt-crack or classical sharp-crack models can be extensively found in [12-16] and [17-21], respectively. In those studies, analytical, semi-analytical or numerical techniques were proposed to solve the associated boundary value problem. It should be remarked that while use of two-dimensional models in the simulation significantly reduces both theoretical and computational efforts, it, at the same time, poses several drawbacks including the loss of out-of-plane information and limited capability to treat cracks of general geometry. Recently, Intarit et al. [22] and Intarit [23] successfully developed an analytical technique based on Hankel integral transforms to investigate the surface stress effect on elastic responses of three-dimensional, nano-sized cracks. Nevertheless, due to the limitation of their solution technique, only penny-shaped cracks under axisymmetric loading can be considered. In practical situations, nano-sized crack problems can be very complex in terms of geometries, loading conditions, and influences to be treated (e.g., surface free energy and residual surface tension). As a result, the development of a fully three-dimensional model and an efficient and powerful numerical procedure to enhance the capability of existing techniques is essential and still requires rigorous investigations. Most recently, Nguyen et al. [24] developed a computational technique by coupling the finite element technique and the boundary integral equation method to model nano-sized planar cracks in an infinite elastic medium. While their technique is applicable to planar cracks of arbitrary shapes, the formulation is still restricted to a limited version of Gurtin-Murdoch model accounting only for the residual surface tension and the implementation was carried out within the context of pure mode-I loading conditions.

The present study directly generalizes the work of Nguyen et al. [24] to incorporate the full Gurtin-Murdoch surface elasticity model (including both the in-plane surface elasticity and the residual surface tension) in modeling the zero-thickness layer. The incorporation of in-plane elasticity of the surface renders the mathematical model more complete and well-suited for studying the influence of in-plane surface stress on essential fracture data such as relative crack-face displacement and near-tip field, and the size-dependent behavior of the predicted solution.

Problem Formulation

In this section, the clear problem description is first stated and then the formulation of the key governing equations for both the bulk material and the zero-thickness layer on the crack surface are briefly summarized. The fully coupled system of governing equations resulting from the enforcement of interfacial conditions is finally presented.

Problem Description

Consider a three-dimensional, infinite medium Ω containing an isolated, planar crack of arbitrary shape with a selected reference Cartesian coordinate system $\{O; x_1, x_2, x_3\}$, as illustrated in Figure 1(a). The crack is represented by two geometrically identical surfaces, denoted by S_c^+ and S_c^- with the corresponding outward unit normal vectors \mathbf{n}^+ and \mathbf{n}^- , and, for convenience in further development, is oriented perpendicular to the x_3 -axis. In the current study, the body force and remote loading are absent and the crack is subjected to prescribed, self-equilibrated, normal tractions \mathbf{t}^{0+} and \mathbf{t}^{0-} on S_c^+ and S_c^- , respectively (see Figure 1(b)). The residual surface tension (τ^s) and the surface Lamé constants λ^s and μ^s of an infinitesimally thin layer on each crack surface are assumed constant whereas the rest of the medium, termed the “*bulk material*”, is made of a homogeneous, isotropic, linear elastic material with shear modulus μ and Poisson’s ratio ν .

A problem statement of the present study is, to determine the complete elastic field including the displacements and stresses within the bulk material by taking the influence of surface stresses into account. Fracture related information such as the relative crack-face displacement and the near-tip stress field is also of primary interest.

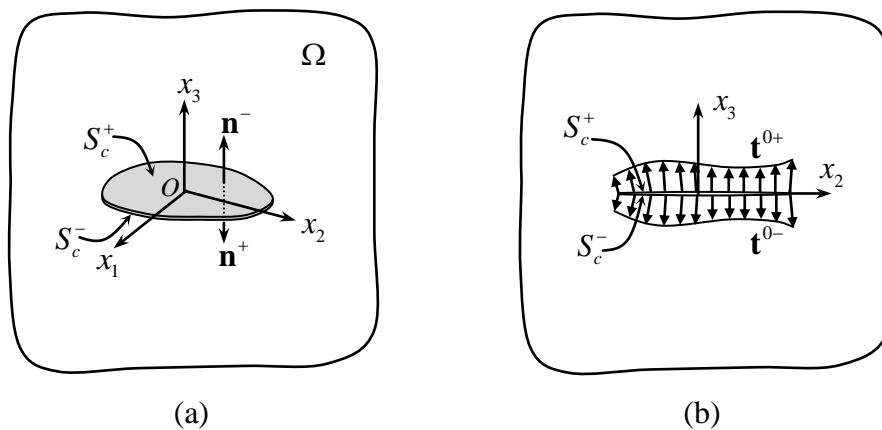


Figure 1. (a) Schematic of planar crack in three-dimensional, linear elastic, infinite medium and (b) prescribed normal traction on crack surfaces

Governing Equations

To form the governing equation of the given problem, the whole medium is first divided into three parts: the bulk material, a zero-thickness layer on the surface S_c^+ , and a zero-

thickness layer on the surface S_c^- . Both the zero-thickness layers are assumed to be fully bonded to the bulk material.

Since the bulk material is made of a linear elastic solid, the classical theory of linear elasticity is used to describe its behavior. For convenience in the treatment of an infinite body containing cracks, the final governing equations are given in terms of boundary integral equations for the sum of the displacements and the jump of the tractions across the crack surface as (see details in Rungamornrat and Mear [28] and Rungamornrat and Senjuntichai [30]),

$$\begin{aligned} \frac{1}{2} \int_{S_c} \tilde{t}_p^\Sigma(\mathbf{y}) u_p^{b\Sigma}(\mathbf{y}) dS(\mathbf{y}) &= \int_{S_c} \tilde{t}_p^\Sigma(\mathbf{y}) \int_{S_c} U_j^p(\boldsymbol{\xi} - \mathbf{y}) t_j^{b\Sigma}(\boldsymbol{\xi}) dS(\boldsymbol{\xi}) dS(\mathbf{y}) \\ &+ \int_{S_c} \tilde{t}_p^\Sigma(\mathbf{y}) \int_{S_c} G_{mj}^p(\boldsymbol{\xi} - \mathbf{y}) D_m u_j^{b\Delta}(\boldsymbol{\xi}) dS(\boldsymbol{\xi}) dS(\mathbf{y}) \\ &- \int_{S_c} \tilde{t}_p^\Sigma(\mathbf{y}) \int_{S_c} H_{ij}^p(\boldsymbol{\xi} - \mathbf{y}) n_i(\boldsymbol{\xi}) u_j^{b\Delta}(\boldsymbol{\xi}) dS(\boldsymbol{\xi}) dS(\mathbf{y}) \end{aligned} \quad (1)$$

$$\begin{aligned} -\frac{1}{2} \int_{S_c} \tilde{u}_k^\Delta(\mathbf{y}) t_k^{b\Delta}(\mathbf{y}) dS(\mathbf{y}) &= \int_{S_c} D_i \tilde{u}_k^\Delta(\mathbf{y}) \int_{S_c} C_{mj}^{tk}(\boldsymbol{\xi} - \mathbf{y}) D_m u_j^{b\Delta}(\boldsymbol{\xi}) dS(\boldsymbol{\xi}) dS(\mathbf{y}) \\ &+ \int_{S_c} D_i \tilde{u}_k^\Delta(\mathbf{y}) \int_{S_c} G_{ik}^j(\boldsymbol{\xi} - \mathbf{y}) t_j^{b\Sigma}(\boldsymbol{\xi}) dS(\boldsymbol{\xi}) dS(\mathbf{y}) \\ &+ \int_{S_c} \tilde{u}_k^\Delta(\mathbf{y}) \int_{S_c} H_{ik}^j(\boldsymbol{\xi} - \mathbf{y}) n_l(\mathbf{y}) t_j^{b\Sigma}(\boldsymbol{\xi}) dS(\boldsymbol{\xi}) dS(\mathbf{y}) \end{aligned} \quad (2)$$

where $S_c \equiv S_c^+$; $D_t(\cdot) = \varepsilon_{mj} n_m \partial(\cdot) / \partial \xi_j$ is a surface differential operator; ε_{mj} is the alternating symbol; $u_j^{b\Sigma} = u_j^{+b} + u_j^{-b}$ and $u_j^{b\Delta} = u_j^{+b} - u_j^{-b}$ are the sum and the jump of the displacements across the crack surface; $t_j^{b\Sigma} = t_j^{+b} + t_j^{-b}$ and $t_j^{b\Delta} = t_j^{+b} - t_j^{-b}$ are the sum and the jump of the tractions across the crack surface; $\{\tilde{t}_p^\Sigma, \tilde{u}_k^\Delta\}$ are sufficiently smooth test functions; and the singular kernels $\{U_j^p, G_{mj}^p, C_{mj}^{tk}, H_{ij}^p\}$ are defined for isotropic linearly elastic materials by,

$$U_j^p(\boldsymbol{\xi} - \mathbf{y}) = \frac{1}{16\pi(1-\nu)\mu r} \left[(3-4\nu)\delta_{pj} + \frac{(\xi_p - y_p)(\xi_j - y_j)}{r^2} \right] \quad (3)$$

$$G_{mj}^p(\boldsymbol{\xi} - \mathbf{y}) = \frac{1}{8\pi(1-\nu)r} \left[(1-2\nu)\varepsilon_{mpj} + \frac{(\xi_p - y_p)(\xi_a - y_a)}{r^2} \varepsilon_{ajm} \right] \quad (4)$$

$$C_{mj}^{tk}(\boldsymbol{\xi} - \mathbf{y}) = \frac{\mu}{4\pi(1-\nu)r} \left[(1-\nu)\delta_{tk}\delta_{mj} + 2\nu\delta_{km}\delta_{tj} - \delta_{kj}\delta_{tm} - \frac{(\xi_k - y_k)(\xi_j - y_j)}{r^2} \delta_{tm} \right] \quad (5)$$

$$H_{ij}^p(\boldsymbol{\xi} - \mathbf{y}) = -\frac{(\xi_i - y_i)\delta_{jp}}{4\pi r^3} \quad (6)$$

where δ_{ij} is the Kronecker delta symbol and $r = \|\boldsymbol{\xi} - \mathbf{y}\|$. The boundary integral Equations (1) and (2) are formulated in a weak form and involve only unknowns on the crack surface. In addition, all involved kernels $\{U_j^p, G_{mj}^p, C_{mj}^{tk}, H_{ij}^p n_i\}$ are only weakly singular of $\mathcal{O}(1/r)$.

The behavior of the two zero-thickness layers is governed by the full version of Gurtin-Murdoch model, including the influence of both the surface elastic constants and the residual surface tension. The equilibrium equations, surface constitutive laws, and strain-

displacement relations of the zero-thickness layers S_c^+ and S_c^- are of the same form and given by (see also [1, 2]),

$$\sigma_{i\beta,\beta}^s + t_i^s + t_i^0 = 0 \quad (7)$$

$$\sigma_{\alpha\beta}^s = \tau^s \delta_{\alpha\beta} + (\lambda^s + \tau^s) \varepsilon_{\gamma\gamma}^s \delta_{\alpha\beta} + 2(\mu^s - \tau^s) \varepsilon_{\alpha\beta}^s + \tau^s u_{\alpha,\beta}^s, \quad \sigma_{3\beta}^s = \tau^s u_{3,\beta}^s \quad (8)$$

$$\varepsilon_{\alpha\beta}^s = \frac{1}{2} (u_{\alpha,\beta}^s + u_{\beta,\alpha}^s) \quad (9)$$

where $\sigma_{i\beta}^s$, $\varepsilon_{\alpha\beta}^s$, u_i^s represent stress, strain and displacement components of each layer; \mathbf{t}^0 denotes prescribed traction on the top of each layer; and \mathbf{t}^s denotes the unknown traction exerted on the interface of each layer by the bulk material. It is noted that the superscript “s” is utilized to emphasize that those quantities are associated with the two layers and Greek subscripts take the values 1, 2 (instead of 1, 2, and 3 as the Latin subscripts). The weak statement of (7)-(9) for both layers S_c^+ and S_c^- can readily be established following a standard procedure based on the weighted residual technique and the final results are given by (see also the development of weak statement for the special case of Gurtin-Murdoch model in the work of Nguyen et al. [24]),

$$\begin{aligned} & \lambda^s \int_{S_c} \tilde{u}_{\alpha,\alpha}^{s\Sigma} u_{\beta,\beta}^{s\Sigma} dS + \frac{\mu^s}{2} \int_{S_c} (\tilde{u}_{\alpha,\beta}^{s\Sigma} + \tilde{u}_{\beta,\alpha}^{s\Sigma}) (u_{\alpha,\beta}^{s\Sigma} + u_{\beta,\alpha}^{s\Sigma}) dS + \tau^s \int_{S_c} \tilde{u}_{3,\beta}^{s\Sigma} u_{3,\beta}^{s\Sigma} dS \\ & - \left[\lambda^s \int_{\partial S_c} \tilde{u}_{\alpha}^{s\Sigma} n_{\alpha} u_{\beta,\beta}^{s\Sigma} d\Gamma + \frac{\mu^s}{2} \int_{\partial S_c} (\tilde{u}_{\alpha}^{s\Sigma} n_{\beta} + \tilde{u}_{\beta}^{s\Sigma} n_{\alpha}) (u_{\alpha,\beta}^{s\Sigma} + u_{\beta,\alpha}^{s\Sigma}) d\Gamma + \tau^s \int_{\partial S_c} \tilde{u}_{3}^{s\Sigma} n_{\beta} u_{3,\beta}^{s\Sigma} d\Gamma \right] \\ & - \int_{S_c} \tilde{u}_i^{s\Sigma} t_i^{s\Sigma} dS = \int_{S_c} \tilde{u}_i^{s\Sigma} t_i^{0\Sigma} dS \end{aligned} \quad (10)$$

$$\begin{aligned} & \lambda^s \int_{S_c} \tilde{u}_{\alpha,\alpha}^{s\Delta} u_{\beta,\beta}^{s\Delta} dS + \frac{\mu^s}{2} \int_{S_c} (\tilde{u}_{\alpha,\beta}^{s\Delta} + \tilde{u}_{\beta,\alpha}^{s\Delta}) (u_{\alpha,\beta}^{s\Delta} + u_{\beta,\alpha}^{s\Delta}) dS + \tau^s \int_{S_c} \tilde{u}_{3,\beta}^{s\Delta} u_{3,\beta}^{s\Delta} dS \\ & - \int_{S_c} \tilde{u}_i^{s\Delta} t_i^{s\Delta} dS = \int_{S_c} \tilde{u}_i^{s\Delta} t_i^{0\Delta} dS \end{aligned} \quad (11)$$

where superscripts “ Σ ” and “ Δ ” indicate the sum and jump of quantities across the crack surfaces and $\tilde{u}_{\alpha}^{s\Sigma}$ and $\tilde{u}_{\alpha}^{s\Delta}$ are sufficiently smooth test functions. It is worth noting that the test function $\tilde{u}_{\alpha}^{s\Delta}$ is chosen to satisfy the homogeneous condition along the crack front similar to the jump of the displacements $u_{\alpha}^{s\Delta}$, i.e., $\tilde{u}_{\alpha}^{s\Delta} = u_{\alpha}^{s\Delta} = 0$ on ∂S_c . By enforcing the continuity of the displacements and tractions along the interface of the two layers and the bulk material (i.e., $u_i^{s\Delta} = u_i^{b\Delta} \equiv u_i^{\Delta}$, $u_i^{s\Sigma} = u_i^{b\Sigma} \equiv u_i^{\Sigma}$, $t_i^{s\Delta} = -t_i^{b\Delta} \equiv -t_i^{\Delta}$, $t_i^{s\Sigma} = -t_i^{b\Sigma} \equiv -t_i^{\Sigma}$), the governing equations of the bulk material (1)-(2) and those of the surfaces (10)-(11) can be combined to obtain a final system of governing equations for the whole medium as,

$$\begin{aligned} \mathcal{A}(\tilde{\mathbf{u}}^{s\Sigma}, \mathbf{u}^{\Sigma}) + \mathcal{B}(\tilde{\mathbf{u}}^{s\Sigma}, \mathbf{t}^{\Sigma}) &= \mathcal{R}_1(\tilde{\mathbf{u}}^{s\Sigma}) \\ \mathcal{B}(\tilde{\mathbf{t}}^{\Sigma}, \mathbf{u}^{\Sigma}) + \mathcal{C}(\tilde{\mathbf{t}}^{\Sigma}, \mathbf{t}^{\Sigma}) + \mathcal{D}(\tilde{\mathbf{t}}^{\Sigma}, \mathbf{u}^{\Delta}) &= 0 \\ \mathcal{D}(\tilde{\mathbf{t}}^{\Sigma}, \tilde{\mathbf{u}}^{\Delta}) + \mathcal{E}(\tilde{\mathbf{u}}^{\Delta}, \mathbf{u}^{\Delta}) &= \mathcal{R}_2(\tilde{\mathbf{u}}^{\Delta}) \end{aligned} \quad (12)$$

where the bilinear integral operators $\mathcal{A}, \mathcal{B}, \mathcal{C}, \mathcal{D}$ and \mathcal{E} are defined by,

$$\mathcal{A}(\mathbf{X}, \mathbf{Y}) = \frac{\lambda^s}{2} \int_{S_c} X_{\alpha,\alpha} Y_{\beta,\beta} dS + \frac{\mu^s}{4} \int_{S_c} (X_{\alpha,\beta} + X_{\beta,\alpha})(Y_{\alpha,\beta} + Y_{\beta,\alpha}) dS + \frac{\tau^s}{2} \int_{S_c} X_{3,\beta} Y_{3,\beta} dS - \left[\frac{\lambda^s}{2} \int_{\partial S_c} X_{\alpha} n_{\alpha} Y_{\beta,\beta} d\Gamma + \frac{\mu^s}{4} \int_{\partial S_c} (X_{\alpha} n_{\beta} + X_{\beta} n_{\alpha})(Y_{\alpha,\beta} + Y_{\beta,\alpha}) d\Gamma + \frac{\tau^s}{2} \int_{\partial S_c} X_3 n_{\beta} Y_{3,\beta} d\Gamma \right] \quad (13)$$

$$\mathcal{B}(\mathbf{X}, \mathbf{Y}) = \frac{1}{2} \int_{S_c} X_p Y_p dS \quad (14)$$

$$\mathcal{C}(\mathbf{X}, \mathbf{Y}) = - \int_{S_c} X_p(\mathbf{y}) \int_{S_c} U_j^p(\xi - \mathbf{y}) Y_j(\xi) dS(\xi) dS(\mathbf{y}) \quad (15)$$

$$\mathcal{D}(\mathbf{X}, \mathbf{Y}) = - \int_{S_c} X_p(\mathbf{y}) \int_{S_c} G_{mj}^p(\xi - \mathbf{y}) D_m Y_j(\xi) dS(\xi) dS(\mathbf{y}) + \int_{S_c} X_p(\mathbf{y}) \int_{S_c} H_{ij}^p(\xi - \mathbf{y}) n_i(\xi) Y_j(\xi) dS(\xi) dS(\mathbf{y}) \quad (16)$$

$$\mathcal{E}(\mathbf{X}, \mathbf{Y}) = - \int_{S_c} D_t X_k(\mathbf{y}) \int_{S_c} C_{mj}^{tk}(\xi - \mathbf{y}) D_m Y_j(\xi) dS(\xi) dS(\mathbf{y}) + \mathcal{F}(\mathbf{X}, \mathbf{Y}) \quad (17)$$

$$\mathcal{F}(\mathbf{X}, \mathbf{Y}) = \frac{\lambda^s}{2} \int_{S_c} X_{\alpha,\alpha} Y_{\beta,\beta} dS + \frac{\mu^s}{4} \int_{S_c} (X_{\alpha,\beta} + X_{\beta,\alpha})(Y_{\alpha,\beta} + Y_{\beta,\alpha}) dS + \frac{\tau^s}{2} \int_{S_c} X_{3,\beta} Y_{3,\beta} dS \quad (18)$$

and the linear integral operators \mathcal{R}_1 and \mathcal{R}_2 are given, in terms of the traction data $\mathbf{t}^{0\Sigma}$ and $\mathbf{t}^{0\Delta}$, by,

$$\mathcal{R}_1(\mathbf{X}) = \frac{1}{2} \int_{S_c} X_l t_l^{0\Sigma} dS \quad (19)$$

$$\mathcal{R}_2(\mathbf{X}) = \frac{1}{2} \int_{S_c} X_l t_l^{0\Delta} dS \quad (20)$$

It is remarked in particular that the last Equation of (12) is obtained by combining Equations (2) and (11), along with choosing the test functions satisfying $\tilde{u}_i^{\Delta} = \tilde{u}_i^{\Delta}$.

Numerical Implementation

Standard procedures for the weakly singular SGBEM (e.g., [25-27, 29]) and for the standard finite element method (e.g., [31-33]) are employed to form the discretized system of linear algebraic equations of (12). Since all involved boundary integrals in the governing equation of the bulk material only contain weakly singular kernels of $\mathcal{O}(1/r)$, standard C^0 interpolation functions are utilized everywhere in the approximation of both trial and test functions.

The construction of the coefficient matrix of the discretized system requires the evaluation of two different types of integrals viz. the single and double surface integrals. The former which contains the regular and well-behaved integrand can be integrated efficiently by standard, low-order Gaussian quadrature, whereas the numerical integration of the latter type (appearing in the governing equations of the bulk part) is more challenging, depending primarily on the behavior of the integrand. Due to the presence of

the singular kernels $\{U_j^p, G_{mj}^p, C_{mj}^{tk}, H_{ij}^p n_i\}$, the integrand becomes weakly singular, nearly singular, and regular when two elements involved in the double surface integrals are identical, relatively close, and sufficiently remote, respectively. The transformation technique and integration rule proposed by Xiao [34] and Li and Han [35] are utilized to treat such double surface integrals. Once the system of linear algebraic equations is solved by a selected efficient linear solver, all the primary unknowns on the crack surface (i.e., $\{u_i^\Delta, u_i^\Sigma, t_i^\Sigma\}$) are obtained and other quantities within the bulk material (e.g., the displacements and stresses) can then be obtained by using integral relations proposed by Rungamornrat and Mear [28].

Results and Discussions

In this section, results for a penny-shaped crack contained in an infinite medium are first presented, to validate the formulation and implementations of the proposed technique with available benchmark solutions. Then, a medium containing an elliptical crack is further investigated, to demonstrate the versatility and robustness of the proposed numerical technique.

In the analysis, three different levels of mesh refinement are adopted to examine the convergence of numerical results. The local region along the crack front is discretized by standard nine-node isoparametric elements whereas the rest of the crack surface is modeled by standard eight-node and six-node isoparametric elements. Young's modulus and Poisson's ratio for the bulk material are taken as $E = 107 \text{ GPa}$ and $\nu = 0.33$, respectively, and elastic constants of the surface and the residual surface tension are chosen identical to those utilized by [22, 23] (i.e., $\lambda^s = 4.4939 \text{ N/m}$, $\mu^s = 2.7779 \text{ N/m}$, $\tau^s = 0.6056 \text{ N/m}$). For convenience in the numerical analysis, all quantities involved in the key governing equation are properly normalized. For instance, the unknown sum of the traction and the prescribed traction on the top surface of the two-thickness layers are normalized by the shear modulus μ (i.e., $t_0^\Sigma = t^\Sigma/\mu$ and $\sigma_{i0} = \sigma_i^0/\mu$); the unknown sum and jump of the relative crack-face displacement are normalized by a special length scale $\Lambda = \kappa^s/\mu = 0.24983 \text{ nm}$ (i.e., $u_0^\Delta = u^\Delta/\Lambda$ and $u_0^\Sigma = u^\Sigma/\Lambda$) where $\kappa^s = |\lambda^s + 2\mu^s|$; and all characteristic lengths representing the geometry of the crack such as the crack radius a , the semi-major axis a , and the semi-minor axis b used in following examples are normalized by the length scale Λ (e.g., $a_0 = a/\Lambda$ and $b_0 = b/\Lambda$).

Penny-Shaped Crack in Elastic Infinite Medium

In order to verify the proposed numerical technique, a special problem of a penny-shaped crack of radius a contained in a three-dimensional, linear elastic, infinite medium (see Figure 2(a)) is fully investigated. The crack is subjected to self-equilibrated, uniformly distributed traction σ^0 normal to its surface. This boundary value problem was previously studied by Intarit et al. [22] and Intarit [23] using Hankel integral transforms along with a solution technique for the dual integral equations, and their results are taken as the benchmark solutions.

The normalized crack opening displacements and vertical stresses near the crack front obtained from the proposed numerical technique for the three meshes shown in Figure 2(b) are presented in Figure 3 along with the benchmark solution generated by [22, 23]. It is seen that the numerical results are slightly mesh dependent and that they are highly accurate and nearly identical to the analytical solution. It can also be pointed out from the results shown in Figure 3 that the two models incorporating the surface stresses with and

without the influence of in-plane surface elasticity yield results significantly different from those predicted by the classical model (i.e., without the surface stress effects). While both the residual surface tension and the in-plane surface elasticity contribute to such discrepancy, the effect of the residual surface tension seems more significant. Similar to previous findings (e.g., [9, 22]), the medium tends to be much stiffer than the classical case, when the full version of the surface stress model is considered in the analysis.

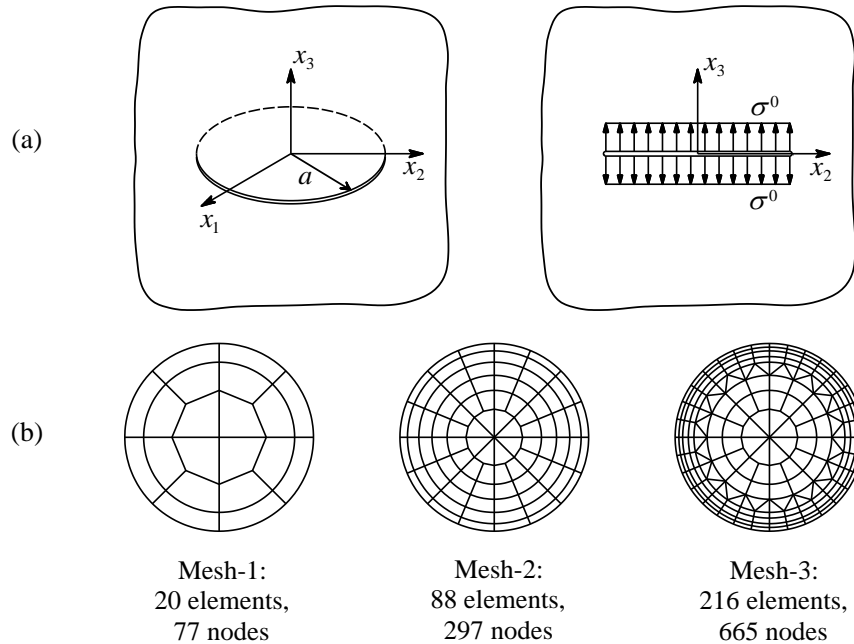


Figure 2. (a) Schematic of penny-shaped crack of radius a embedded in a three-dimensional, isotropic, linear elastic, infinite medium under self-equilibrated, uniformly distributed, normal traction and (b) three meshes used in numerical study

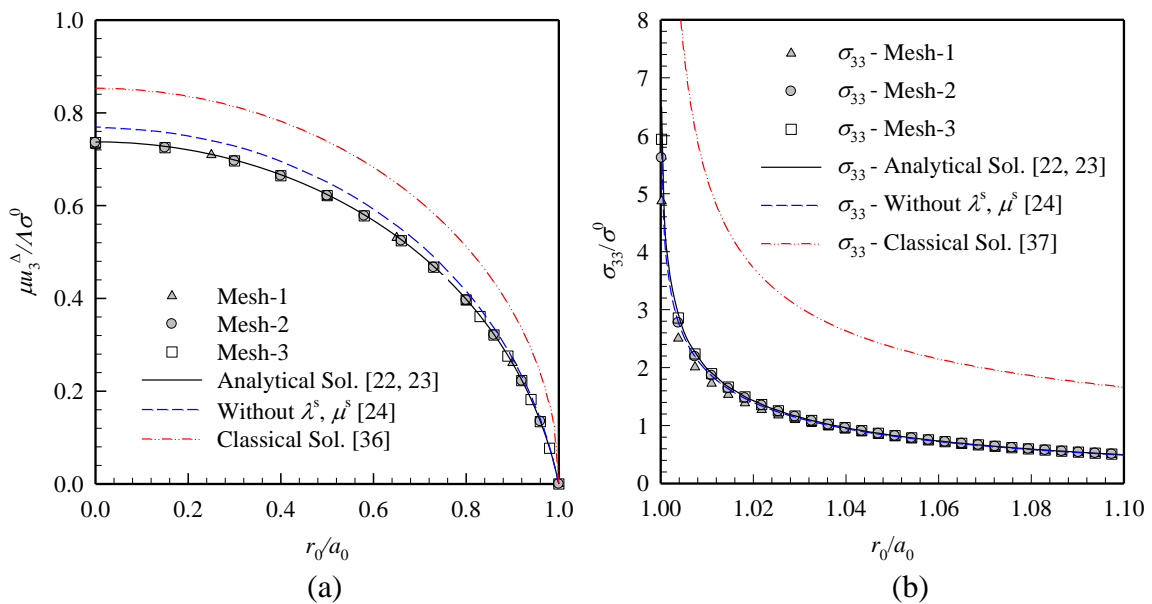


Figure 3. Results for penny-shaped crack under uniformly distributed normal traction; (a) normalized crack opening displacement and (b) normalized vertical stress along the x_1 -axis where $r_0 = x_1/\Lambda$

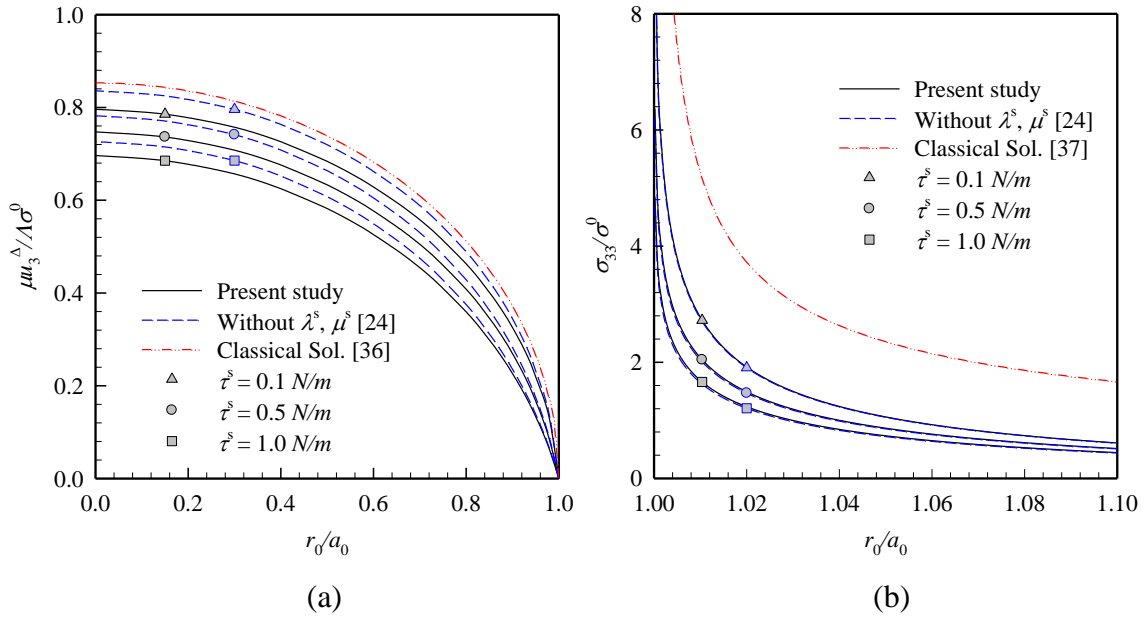


Figure 4. Results for penny-shaped crack under uniformly distributed normal traction for different residual surface tension τ^s varied from 0 to 1 N/m and $E = 107$ GPa, $\nu = 0.33$, $\lambda^s = 4.4939$ N/m, $\mu^s = 2.7779$ N/m; (a) normalized crack opening displacement and (b) normalized vertical stress along the x_1 -axis where $r_0 = x_1/\Lambda$

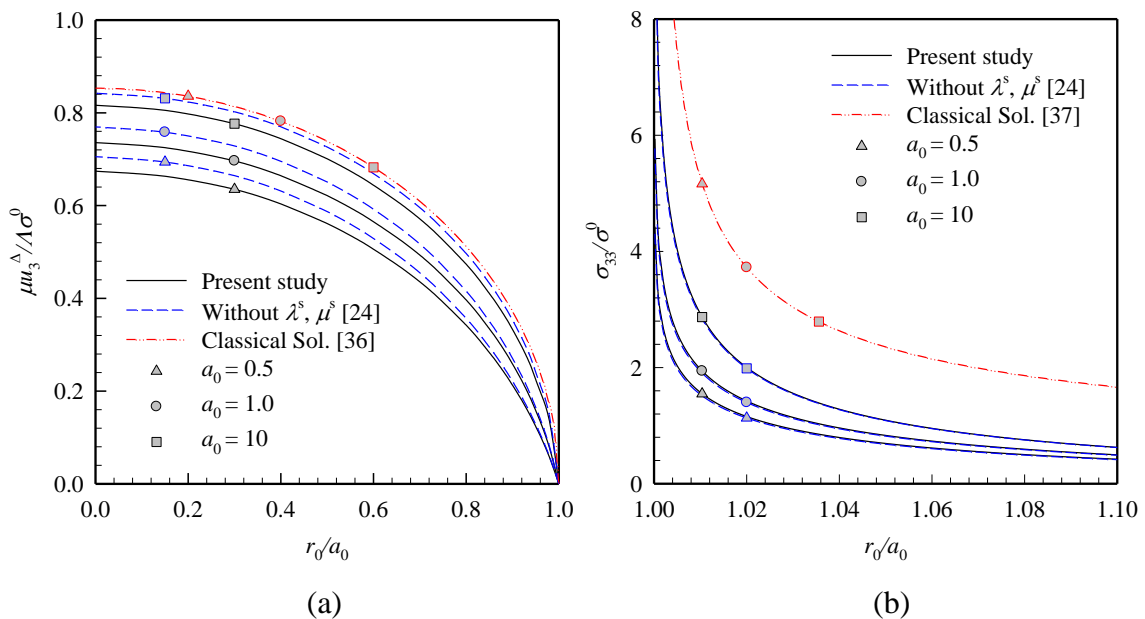


Figure 5. Results for penny-shaped crack under uniformly distributed normal traction for different crack radii $a_0 \in \{0.5, 1.0, 10.0\}$ and $E = 107$ GPa, $\nu = 0.33$, $\lambda^s = 4.4939$ N/m, $\mu^s = 2.7779$ N/m, $\tau^s = 0.6056$ N/m; (a) normalized crack opening displacement and (b) normalized vertical stress along the x_1 -axis where $r_0 = x_1/\Lambda$

To further examine the influence of the residual surface tension on the normalized crack opening displacements and vertical stresses near the crack boundary when the

surface elasticity is included, results are presented in Figure 4 for various values of the residual surface tension τ^s ranging from 0 to 1.0 N/m with the surface elastic constants remaining fixed. It is evident that the residual surface tension exhibits significant influence on both the crack opening displacement and the vertical stress in the local region near the crack front. As τ^s becomes larger, the deviation of results from the classical case (i.e., without the surface stresses) increases significantly.

To demonstrate the size-dependent characteristics of results owing to the presence of surface stresses, the normalized crack opening displacement and vertical stresses near the crack front obtained from three models (i.e., the classical model without the surface stresses, the model incorporating only the residual surface tension [24], and the current model) are shown in Figure 5 for three different crack radii $a_0 = a / \Lambda \in \{0.5, 1.0, 10.0\}$. It is evident from this particular set of results that solutions predicted by the two models including surface stresses clearly exhibit size-dependent behavior, whereas those predicted by the classical model are size-independent. Furthermore, as the crack radius decreases, the effect of surface stresses is more significant, especially when the in-plane surface elasticity is included.

In addition, the incorporation of in-plane surface elasticity further reduces the crack opening displacement (see Figure 4(a) and Figure 5(a)). However, the existence of such surface elastic constants does not significantly influence the vertical stresses in the vicinity of the crack front. The discrepancy of predicted vertical stresses near the crack front from the two models with and without the surface elastic constants is barely recognizable (see Figure 4(b) and Figure 5(b)).

Elliptical Crack in an Elastic Infinite Medium

To demonstrate the capability of the developed numerical technique of treating cracks of arbitrary shape, a problem associated with a three-dimensional, linear elastic, infinite medium containing an elliptical crack is considered (see Figure 6(a)). The crack front is described, in terms of a parameter t , by,

$$x_1 = a \cos t, \quad x_2 = b \sin t, \quad x_3 = 0; \quad t \in [0, 2\pi] \quad (21)$$

where a and b denote the major semi-axis and the minor semi-axis of the crack, respectively. The crack is subjected to a self-equilibrated, uniformly distributed normal traction σ^0 . Numerical results are reported for three different aspect ratios $a/b \in \{1, 2, 3\}$ and three meshes shown in Figure 6(b) are adopted in the numerical study.

The normalized crack opening displacement and vertical stress along the minor axis, with the influence of the surface stresses, are presented in Figure 7 for all three aspect ratios considered. It can be seen from results in Figure 7, that when the aspect ratio a/b increases, the effect of the surface stresses on the crack opening displacement and the near-tip vertical stresses decreases. To further examine the size-dependent characteristics of results owing to the effect of surface stresses, the crack opening displacement and the vertical stresses near the crack front for $b_0 = b / \Lambda \in \{0.5, 1.0, 10.0\}$ and for the aspect ratio $a/b = 2$ are shown in Figure 8. It can be observed from these results that the normalized crack opening displacement and the vertical stresses in the neighborhood of the crack front are apparently size-dependent. This is in contrast to the classical model (i.e., without the surface stresses) whose predicted solutions are size-independent. When the crack-size decreases, the influence of surface stresses becomes significant; in particular, it renders the medium much stiffer. Additionally, in agreement with the previous example, it can also be

observed that in-plane surface elasticity further reduced the crack opening displacement. However, it has negligible influence on the vertical stresses near the crack front.

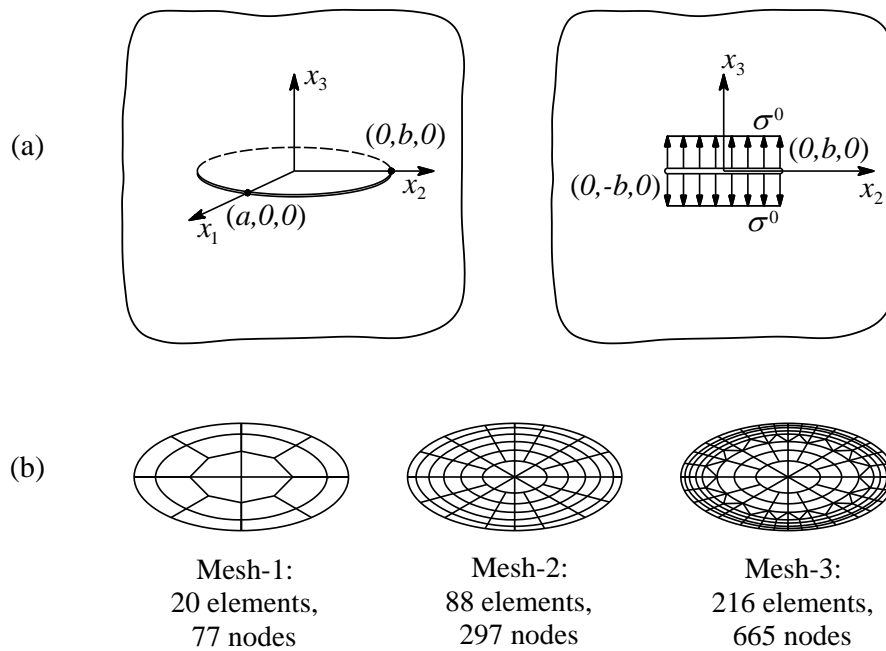


Figure 6. (a) Schematic of elliptical crack in three-dimensional, isotropic, linear elastic infinite medium under self-equilibrated, uniformly distributed, normal traction and (b) three meshes used in numerical study

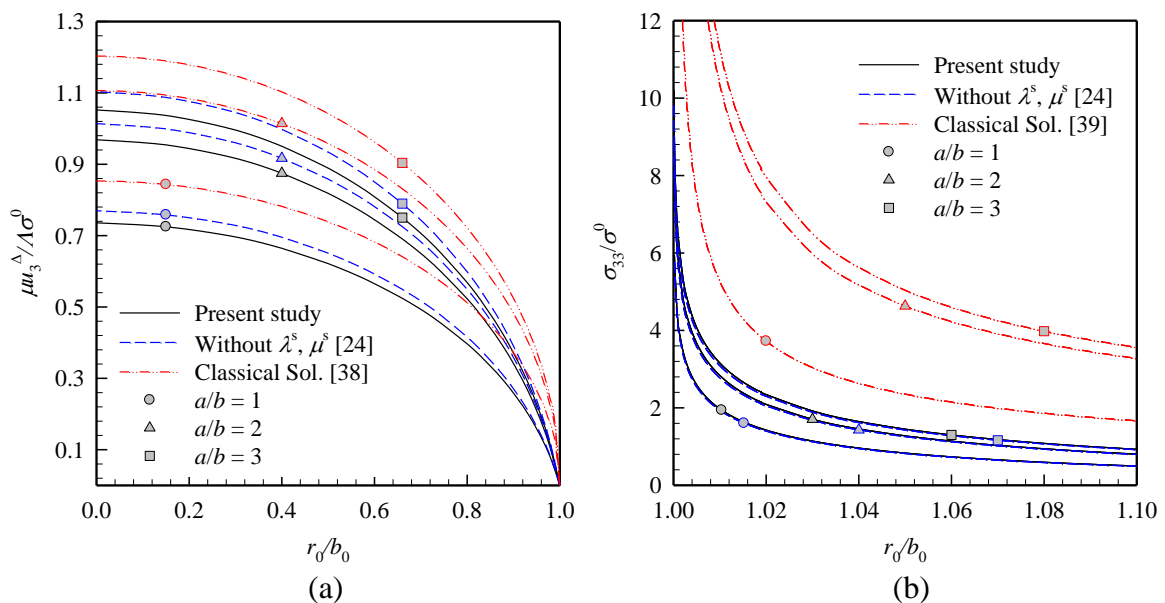


Figure 7. Results for elliptical crack under uniformly distributed normal traction and for different aspect ratios $a/b \in \{1, 2, 3\}$; (a) normalized crack opening displacement along the minor axis and (b) normalized vertical stress near the crack front along the minor axis

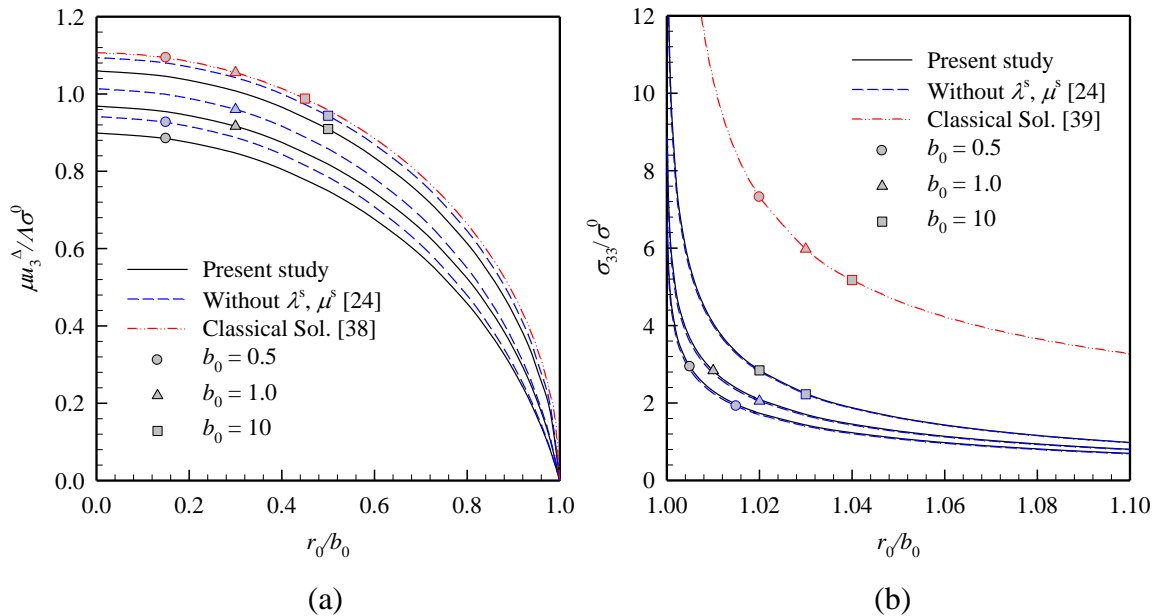


Figure 8. Results for elliptical crack under uniformly distributed normal traction for different crack radii $b_0 \in \{0.5, 1.0, 10.0\}$ and $a/b = 2$; (a) normalized crack opening displacement along the minor axis and (b) normalized vertical stress near the crack front along the minor axis

Conclusions

A numerical technique has been established for modeling planar cracks in three-dimensional, linear elastic media including the surface stress effect. The governing equations have been formulated using the conventional theory of isotropic linear elasticity for the bulk medium and the full version of surface constitutive relation proposed by Gurtin and Murdoch for the infinitesimally thin layers on the crack surfaces. The full coupled system of governing equations has been solved numerically by using the FEM-SGBEM coupling procedure. The numerical results for a penny-shaped crack problem have been benchmarked with the available analytical solution, to verify the formulation and the proposed FEM-SGBEM technique. Results for an elliptical crack have also been investigated, to demonstrate the ability of the proposed computational procedure to treat cracks of arbitrary shape. The numerical technique developed in the present study has been found computationally promising and capable of modeling planar nano-sized cracks with arbitrary shape. Although results are presented only for the single crack problem for the sake of brevity, the formulation and implementation are definitely applicable to problems of multiple cracks. From an extensive numerical study, the significant role of the surface stresses and the size-dependent characteristics of the predicted solutions are confirmed. In particular, a model including both in-plane elasticity of the surface and residual surface tension, significantly increases the near-surface material stiffness and predicts a much lower crack opening displacement and near-tip vertical stress, in comparison with the classical solution.

Acknowledgement

Financial support from JICA AUN/SEED-Net Scholarship and Thailand Research Fund (Grant No. MRG5380159 and Grant No. BRG5480006) are gratefully acknowledged.

References

- [1] M.E. Gurtin, and A.I. Murdoch, "A continuum theory of elastic material surfaces," *Archive for Rational Mechanics and Analysis*, Vol. 57, No. 4, pp. 291-323, 1975.
- [2] M.E. Gurtin, and A.I. Murdoch, "Surface stress in solids," *International Journal of Solids and Structures*, Vol. 14, No. 6, pp. 431-440, 1978.
- [3] L.H. He, C.W. Lim, and B.S. Wu, "A continuum model for size-dependent deformation of elastic films of nano-scale thickness," *International Journal of Solids and Structures*, Vol. 41, No. 3-4, pp. 847-857, 2004.
- [4] R. Dingreville, J. Qu, and M. Cherkaoui, "Surface free energy and its effect on the elastic behavior of nano-sized particles, wires and films," *Journal of the Mechanics and Physics of Solids*, Vol. 53, No. 8, pp. 1827-1854, 2005.
- [5] D.W. Huang, "Size-dependent response of ultra-thin films with surface effects," *International Journal of Solids and Structures*, Vol. 45, No. 2, pp. 568-579, 2008.
- [6] L. Tian, and R.K.N.D. Rajapakse, "Finite element modeling of nanoscale inhomogeneities in an elastic matrix," *Computational Materials Science*, Vol. 41, No. 1, pp. 44-53, 2007.
- [7] L. Tian, and R.K.N.D. Rajapakse, "Analytical solution for size-dependent elastic field of a nanoscale circular inhomogeneity," *ASME Journal of Applied Mechanics*, Vol. 74, No. 3, pp. 568-574, 2007.
- [8] L. Tian, and R.K.N.D. Rajapakse, "Elastic field of an isotropic matrix with a nanoscale elliptical inhomogeneity," *International Journal of Solids and Structures*, Vol. 44, No. 24, pp. 7988-8005, 2007.
- [9] Y. Pinyochotiwong, J. Rungamornrat, and T. Senjuntichai, "Rigid frictionless indentation on elastic half space with influence of surface stresses," *International Journal of Engineering Science*, Vol. 71, No. 0, pp. 15-35, 2013.
- [10] R.E. Miller, and V.B. Shenoy, "Size-dependent elastic properties of nanosized structural elements," *Nanotechnology*, Vol. 11, No. 3, pp. 139-147, 2000.
- [11] V.B. Shenoy, "Size-dependent rigidities of nanosized torsional elements," *International Journal of Solids and Structures*, Vol. 39, No. 15, pp. 4039-4052, 2002.
- [12] G.F. Wang, X.Q. Feng, T.J. Wang, and W. Gao, "Surface effects on the near-tip stresses for mode-I and mode-III cracks," *ASME Journal of Applied Mechanics*, Vol. 75, No. 1, pp. 011001-011005, 2008.
- [13] X.L. Fu, G.F. Wang, and X.Q. Feng, "Surface effects on the near-tip stress fields of a mode-II crack," *International Journal of Fracture*, Vol. 151, No. 2, pp. 95-106, 2008.
- [14] X.L. Fu, G.F. Wang, and X.Q. Feng, "Surface effects on mode-I crack tip fields: A numerical study," *Engineering Fracture Mechanics*, Vol. 77, No. 7, pp. 1048-1057, 2010.
- [15] Q.H. Fang, Y.Liu, Y.W. Liu, and B.Y. Huang, "Dislocation emission from an elliptically blunted crack tip with surface effects," *Physica B: Condensed Matter*, Vol. 404, No. 20, pp. 3421-3424, 2009.
- [16] G.F. Wang, and Y. Li, "Influence of surface tension on mode-I crack tip field," *Engineering Fracture Mechanics*, Vol. 109, No. 0, pp. 290-301, 2013.
- [17] C.I. Kim, P. Schiavone, and C.Q. Ru, "Analysis of a mode-III crack in the presence of surface elasticity and a prescribed non-uniform surface traction," *Zeitschrift für angewandte Mathematik und Physik*, Vol. 61, No. 3, pp. 555-564, 2010.
- [18] C.I. Kim, P. Schiavone, and C.Q. Ru, "The effect of surface elasticity on a mode-III interface crack," *Archives of Mechanics*, Vol. 63, No. 3, pp. 267-286, 2011.
- [19] C.I. Kim, P. Schiavone, and C.Q. Ru, "Analysis of plane-strain crack problems (Mode-I & Mode-II) in the presence of surface elasticity," *Journal of Elasticity*, Vol. 104, No. 1, pp. 397-420, 2011.

- [20] H. Nan, and B. Wang, "Effect of residual surface stress on the fracture of nanoscale materials," *Mechanics Research Communications*, Vol. 44, pp. 30-34, 2012.
- [21] H.S. Nan, and B.L. Wang, "Effect of crack face residual surface stress on nanoscale fracture of piezoelectric materials," *Engineering Fracture Mechanics*, Vol. 110, pp. 68-80, 2013.
- [22] P. Intarit, T. Senjuntichai, J. Rungamornrat, and R.K.N.D. Rajapakse, "Stress analysis of penny-shaped crack considering the effects of surface elasticity," In: *Proceedings of 20th Annual International Conference on Composites or Nano Engineering (ICCE-20)*, Ramada Beijing North Hotel, Beijing, P.R. China, 2012.
- [23] P. Intarit. *Solutions of Elastic Medium with Surface Stress Effects*. Thesis (PhD), Chulalongkorn University, Bangkok, Thailand, 2013.
- [24] T.B. Nguyen, J. Rungamornrat, T. Senjuntichai, and A.C. Wijeyewickrema, "FEM-SGBEM coupling for modeling of mode-I planar cracks in three-dimensional elastic media with residual surface tension effects," *Engineering Analysis with Boundary Elements* (under review), 2013.
- [25] S. Li, and M.E. Mear, "Singularity-reduced integral equations for displacement discontinuities in three-dimensional linear elastic media," *International Journal of Fracture*, Vol. 93, pp. 87-114, 1998.
- [26] S. Li, M.E. Mear, and L. Xiao, "Symmetric weak-form integral equation method for three-dimensional fracture analysis," *Computer Methods in Applied Mechanics and Engineering*, Vol. 151, pp. 435-459, 1998.
- [27] J. Rungamornrat, "Analysis of 3D cracks in anisotropic multi-material domain with weakly singular SGBEM," *Engineering Analysis with Boundary Elements*, Vol. 30 , No. 10, pp. 834-846, 2006.
- [28] J. Rungamornrat, and M.E. Mear, "Weakly-singular, weak-form integral equations for cracks in three-dimensional anisotropic media," *International Journal of Solids and Structures*, Vol. 45, No. 5, pp. 1283-1301, 2008.
- [29] J. Rungamornrat, and M.E. Mear, "A weakly-singular SGBEM for analysis of cracks in 3D anisotropic media," *Computer Methods in Applied Mechanics and Engineering*, Vol. 197, pp. 4319-4332, 2008.
- [30] J. Rungamornrat, and T. Senjuntichai, "Regularized boundary integral representations for dislocations and cracks in smart media," *Smart Materials and Structures*, Vol. 18, No. 074010, p. 14, 2009.
- [31] K.J. Bathe, *Finite Element Procedures*, Prentice-Hall, New Jersey, 1990.
- [32] T.J.R. Hughes, *The Finite Element Method: Linear Static And Dynamic Finite Element Analysis*, Dover Publications, New Jersey, 2000.
- [33] O.C. Zienkiewicz, and R.L. Taylor, *The Finite Element Method: Solid Mechanics*, Vol. 2, Butterworth-Heinemann, Oxford, 2000.
- [34] L. Xiao. *Symmetric Weak-Form Integral Equation Method For Three-Dimensional Fracture Analysis*, Thesis (PhD), The University of Texas at Austin, Texas, 1998.
- [35] H.B. Li, and G.M. Han, "A new method for evaluating singular integral in stress analysis of solids by the direct boundary element method," *International Journal for Numerical Methods in Engineering*, Vol. 21, pp. 2071-2098, 1985.
- [36] H. Tada, P.C. Paris, and G.R. Irwin, *The Stress Analysis of Cracks Handbook*, American Society of Mechanical Engineers, 2000.
- [37] M.K. Kassir, and G.C. Sih, *Three-Dimensional Crack Problems: A New Selection of Crack Solutions in Three-dimensional Elasticity*, Vol. 2, Noordhoff International Publishing, Leyden, 1975.

- [38] C. Zeng-shen, "Discussion on the SIF for points on border of elliptical flat crack inside infinite solid under uniform tension," *Applied Mathematics and Mechanics*, Vol. 3, No. 4, pp. 521-526, 1982.
- [39] A.E. Green, and I.N. Sneddon, "The distribution of stress in the neighborhood of a flat elliptical crack in an elastic solid," *Mathematical Proceedings of the Cambridge Philosophical Society*, Vol. 46, No. 1, pp. 159–163, 1950.